International Journal for Modern Trends in Science and Technology
Volume 11, Issue 05, pages 1224-1236
ISSN: 2455-3778 online
Available online at: http://www.ijmtst.com/vol11issue05.html
DOI: https://doi.org/10.5281/zenodo.15511558

Bidirectional Wireless Power Transfer for High and Low-Voltage EV Charging in a Hybrid Solar-Grid System Using Shared Converter and Magnetic Coupler

Ashok Kumar.M[1], A. Rajesh[2], Dr. K. Siva Kumar [3]

[1]PG Student, Dept. of Electrical & Electronics Engineering, Sri Venkatesa Perumal College of Engineering and Technology, Puttur, Andhra Pradesh, India
[2]Assistant Professor, Dept. of Electrical & Electronics Engineering, Sri Venkatesa Perumal College of Engineering and Technology, Puttur, Andhra Pradesh, India
[3]Professor, Dept. of Electrical & Electronics Engineering, Sri Venkatesa Perumal College of Engineering and Technology, Puttur, Andhra Pradesh, India

To Cite this Article
Ashok Kumar.M, A. Rajesh & Dr. K. Siva Kumar (2025). Bidirectional Wireless Power Transfer for High and Low-Voltage EV Charging in a Hybrid Solar-Grid System Using Shared Converter and Magnetic Coupler. International Journal for Modern Trends in Science and Technology, 11(05), 1224-1236. https://doi.org/10.5281/zenodo.15511558

Article Info
Received: 27 April 2025; Accepted: 22 May 2025.; Published: 25 May 2025.

KEYWORDS

Electric Vehicle Charging, Bidirectional Wireless Power Transfer, High-Voltage Battery, Low-Voltage Battery, Solar Photovoltaic System, Maximum Power Point Tracking, dq0 Control, Vehicle-to-Grid, Vehicle-to-Vehicle.

ABSTRACT

This paper proposes a novel bidirectional wireless power transfer (WPT) system for electric vehicle (EV) charging at both high-voltage (HV) and low-voltage (LV) levels within a hybrid solar-grid energy framework. The system integrates a solar photovoltaic (PV) array and grid connection to ensure reliable, efficient, and flexible EV charging. A shared power converter combined with a magnetic coupler enables seamless wireless energy transfer, supporting power flow from grid to EV and EV to EV. The solar PV system employs a DC-DC boost converter with a Perturb and Observe (P&O) maximum power point tracking (MPPT) algorithm to maximize renewable energy extraction under varying environmental conditions. The grid interface utilizes a bidirectional AC-DC voltage source converter controlled through a dq0 reference frame method to regulate active and reactive power, thereby maintaining grid stability, power quality, and frequency synchronization. An auxiliary power module facilitates energy transfer between HV and LV EVs, enhancing operational flexibility and enabling inter-vehicle power sharing. This feature enhances energy flexibility and offers a solution for off-grid or emergency charging scenarios. Simulation results demonstrate the system's effectiveness in optimizing solar energy use,

minimizing grid dependency, and ensuring stable operation under diverse load and generation scenarios. This integrated approach offers a promising solution for sustainable, resilient, and flexible EV charging infrastructure.

1. Introduction

The growing demand for electric vehicles (EVs) has driven rapid advancements in power electronics, renewable energy integration, and smart charging infrastructure. As global transportation sectors shift toward electrification to reduce carbon emissions and fossil fuel dependency, innovative EV charging solutions are needed to ensure flexibility, reliability, and sustainability [1][2]. Traditional wired charging systems, although widely used, face challenges related to user convenience, insulation degradation, safety risks, and wear and tear on physical connectors [3][4]. In response, wireless power transfer (WPT) has emerged as a promising technology, offering contactless energy transmission with improved user experience, operational safety, and compatibility with autonomous charging environments [5][6]. Recent developments in WPT systems focus on enhancing power transfer efficiency, alignment tolerance, and bidirectional energy flow capabilities. Magnetic resonant coupling, particularly in the form of inductive and capacitive techniques, has shown significant promise for EV charging applications due to its medium-range efficiency and scalability [7][8]. Researchers have proposed various coil configurations, compensation topologies, and control algorithms to improve the coupling efficiency under dynamic and static conditions [9][10]. Bidirectional WPT, in particular, plays a pivotal role in enabling not only grid-to-vehicle (G2V) charging but also vehicle-to-grid (V2G), vehicle-to-home (V2H), and vehicle-to-vehicle (V2V) energy transfers, thereby transforming EVs into distributed energy storage assets [11][12]. The integration of renewable energy sources, such as solar photovoltaic (PV) systems, into EV charging infrastructure addresses key issues related to environmental sustainability and grid dependency [13][14]. Solar PV is widely recognized for its accessibility, modularity, and eco-friendliness, making it a suitable candidate for both centralized and decentralized EV charging setups [15]. However, the intermittent and nonlinear nature of solar irradiance demands efficient power regulation and real-time control strategies. Maximum power point tracking (MPPT) algorithms such as Perturb and Observe (P&O) have been widely adopted for optimizing energy extraction from PV systems under varying atmospheric conditions [16][17]. These algorithms ensure that the system operates at the optimal voltage and current levels to extract the maximum power from the PV source. To effectively utilize both renewable and grid energy for EV charging, advanced bidirectional power converters are employed. Voltage Source Converters (VSCs) controlled using dq0 transformation enable active and reactive power control, synchronization with the grid, and power quality enhancement [18][19]. These converters also facilitate energy export during V2G and emergency power scenarios. Shared power electronic architectures further reduce cost, size, and complexity by integrating both high-voltage (HV) and low-voltage (LV) battery modules through a unified converter and magnetic coupling interface [20][21]. Such architectures enable simultaneous or alternate charging of traction batteries and auxiliary battery systems, improving system compactness and operational flexibility [22]. Dual-voltage EV architectures are increasingly prevalent in modern vehicles, with the high-voltage battery supporting propulsion and the low-voltage battery powering auxiliary systems such as lighting, control units, and infotainment [23]. Conventional charging systems typically rely on separate charging modules for each battery pack, leading to increased hardware complexity and inefficiency. To overcome these limitations, recent research has focused on shared coupling topologies and modular converters capable of handling both voltage levels within a single integrated system [24][25]. These designs improve thermal management, reduce electromagnetic interference, and enhance overall power conversion efficiency. Moreover, such shared systems support energy balancing between HV and LV modules, allowing surplus energy from the propulsion battery to charge the auxiliary battery, or vice versa, depending on system conditions. In addition to technical advancements, bidirectional EV charging systems contribute to grid resilience and disaster recovery efforts. During emergencies or off-grid scenarios, V2V or V2H power transfer can provide critical energy to nearby vehicles or buildings [26][27]. Wireless EV-to-EV charging systems allow for mobile

power exchange without the need for specialized cabling or infrastructure, enhancing usability in remote or damaged areas. Moreover, these systems can be coordinated with intelligent control algorithms and Internet of Things (IoT) frameworks to facilitate energy dispatch, scheduling, and priority-based charging operations [28]. Despite these advancements, the literature reveals a lack of unified frameworks that seamlessly integrate solar PV generation, grid power, and bidirectional WPT for HV and LV EV charging in a single architecture. Existing studies often focus on either renewable integration, wireless charging, or bidirectional converters in isolation. Very few systems propose a shared converter and coupler design capable of dynamically switching between G2V, V2G, and V2V operational modes under varying energy availability and load demands. Furthermore, coordinated control of MPPT, VSC, and WPT modules in real time remains underexplored, especially in multi-battery EV systems with flexible energy flow paths. This paper aims to address these gaps by presenting a novel bidirectional WPT system for EVs that integrates solar PV, grid power, and dual-battery support using a shared converter and magnetic coupler configuration. The proposed system leverages a P&O MPPT algorithm for solar optimization, a dq0-based VSC for grid interfacing, and a wireless energy transfer framework capable of managing HV-LV energy flows. This feature enhances energy flexibility and offers a solution for off-grid or emergency charging scenarios. The system is validated through simulation, demonstrating improved energy utilization, reduced grid stress, and enhanced resilience for future EV charging applications.

2. System Configuration

The proposed system integrates solar PV and grid energy sources to enable efficient and flexible dual-level EV charging via wireless power transfer (WPT). A DC-DC boost converter, controlled by a Perturb and Observe (P&O) MPPT algorithm, ensures maximum power extraction from the solar PV array under variable irradiance conditions. The harvested power is supplied to the EVs through a shared power converter and magnetic coupler that facilitate wireless energy transfer. When solar power is sufficient, the system prioritizes renewable energy for EV charging as shown in Fig.1. During periods of low solar generation, a bidirectional AC-DC voltage source converter (VSC) connected to the grid compensates for the shortfall. This VSC operates under a dq0 control strategy to regulate active and reactive power, maintain grid frequency, and ensure power quality. A key feature of the system is the auxiliary power module, which supports both high-voltage and low-voltage EVs. It also enables EV-to-EV wireless power transfer, allowing energy sharing from a high-voltage EV to a low-voltage EV. This enhances system flexibility and provides a practical solution for off-grid or emergency charging situations.

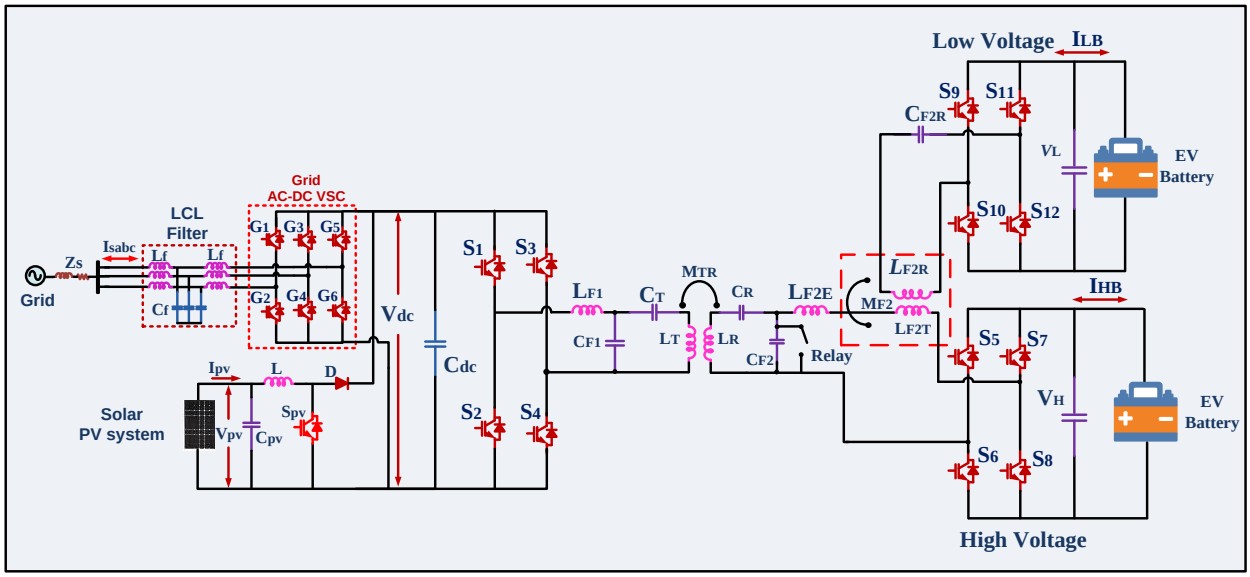

Fig. 1 proposed solar PV and integrating with grid system configuration

3. PROPOSED INTEGRATION METHOD

A. Modeling of Solar PV Configuration

A single diode solar cell converts sunlight into electrical energy using the photovoltaic effect. When sunlight strikes the surface of the solar cell, photons generate electron-hole pairs, creating a photocurrent. This current flows through an external circuit and contributes to power generation as shown in Fig.2. The core element of the solar cell is a p-n junction represented by a diode in the equivalent circuit, which controls the direction of current flow. The output characteristics are influenced by two key parasitic elements: series resistance (Rs) and shunt resistance (Rsh). The series resistance reduces voltage due to resistive losses, while shunt resistance causes leakage current that decreases output power. The V-I (voltage-current) characteristics curve of a solar cell starts at short-circuit current (Isc) when voltage is zero and ends at open-circuit voltage (Voc) when current is zero. The curve is non-linear due to the exponential nature of the diode current. The point on the curve where the product of voltage and current is maximum is known as the Maximum Power Point (MPP), and operating the solar cell at this point ensures maximum energy extraction as shown in Fig.3. Since MPP varies with sunlight intensity and temperature, Maximum Power Point Tracking (MPPT) algorithms are used in practice to dynamically adjust operating conditions and enhance system performance.

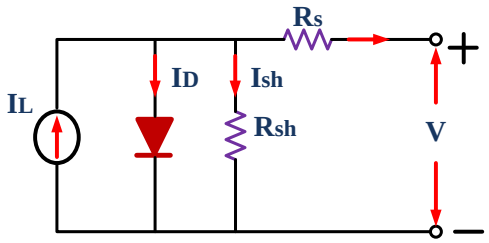

Fig. 2 single diode equivalent model of PV solar

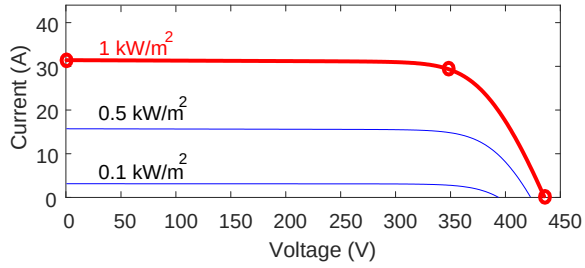

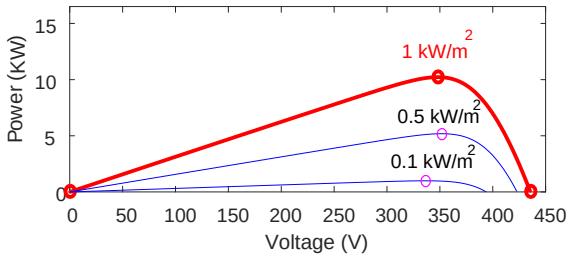

Fig.3 VI characteristics of solar PV panel

Photovoltaic (PV) energy is clean, inexhaustible and free to harvest. Regardless of intermittency of sunlight solar energy is widely used to generate direct current (DC) from sun intensity. The flow occurs when the photo conductive cell is connected to the external load. PV array has nonlinear characteristics so it is necessary to model it for the design and simulation of MPPT for PV application. The most standard modeling approaches in solar PV are a single diode and double diode demonstration. Single diode show is least composite and less composite, but to enhance the exactness of the PV demonstrating, dual diode models are even chosen. Despite the statistic that the twice diode display has high difficulty and also computational problem within the abstraction of parameters. For solar PV array model represented in electrical equivalent circuit exposed in Fig. 4. The yield equation of solitary diode model is

$$I = I_{Ph} - I_0\left[\exp\left(\frac{V+IR_s}{nV_T}\right) - 1\right] - \left(\frac{V+IR_s}{R_{sh}}\right) \quad (1)$$

And thermal voltage is given by

$$V_T = \frac{KT}{q} \quad (2)$$

$$I_d = I_o\left(e^{qVd/nKT} - 1\right) \quad (3)$$

$$I = I_{PV} - I_d - I_{sh} \quad (4)$$

$$I_{sh} = \left(V + \frac{IR_s}{R_{sh}}\right) \quad (5)$$

$$I_{PV} = I - I_o\left[\exp\left(\frac{KV}{n_s}\right) - 1\right] \quad (6)$$

Reverse saturation current

$$I_o = n_s I_{PV} - n_s I_{rs}\left[\exp\left(\frac{KV}{n_s}\right) - 1\right] \quad (7)$$

$$P_{\max} = V_{oc} \times I_{sc} \quad (8)$$

$$P_{mpp} = v_{mp} \times I_{mp} \quad (9)$$

B. Solar PV Boost Converter

A solar boost converter is a DC to DC power electronic device used to increase the voltage output from a solar photovoltaic panel to a higher level that is suitable for charging batteries or powering loads. Since the voltage generated by a solar panel is often lower than what is needed for many applications, a boost converter plays a vital role in ensuring the system delivers adequate voltage. The converter functions by rapidly switching a

semiconductor device on and off, allowing energy to be stored in an inductor during the on phase. When the switch is turned off, the stored energy in the inductor is released to the output through a diode, resulting in a voltage that is higher than the input. The process is governed by pulse-width modulation which adjusts the duration of the on and off states to regulate the output voltage. To enhance energy harvesting, a maximum power point tracking algorithm such as the perturb and observe method is often employed as shown in Fig.5. This algorithm continuously adjusts the operating point of the solar panel to extract the maximum available power under varying sunlight and temperature conditions. The integration of the boost converter with MPPT improves the overall efficiency and stability of the solar energy system.

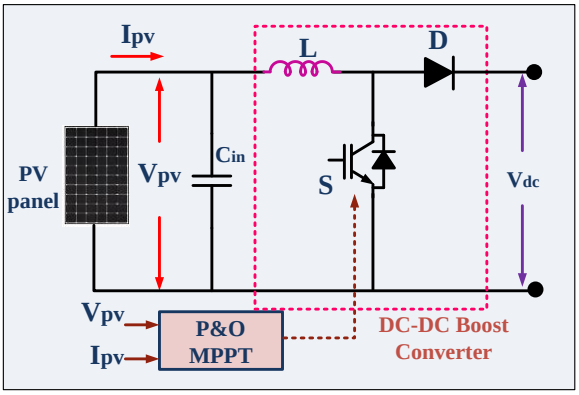

Fig. 4 solar PV P&O MPPT DC-DC boost converter

Duty ratio for Boost converter, the expression is given by

$$D = 1 - \frac{V_{in} \times \eta}{V_{out}} \quad (10)$$

Ripple current expression is given by

$$\Delta I_L = \frac{V_{in} \times D}{f_s \times L} \quad (11)$$

Inductor equation is given by

$$L = \frac{V_{in} \times (V_{out} - V_{in})}{\Delta I_L \times f_s \times V_{out}} \quad (12)$$

Capacitor equation is given by

$$C = \frac{I_{out} \times D}{f_s \times \Delta V_{out}} \quad (13)$$

C. Perturb and Observe (P&O) algorithm

The Perturb and Observe (P&O) algorithm is a widely used technique to track the Maximum Power Point (MPP) in solar photovoltaic (PV) systems. The main idea behind the P&O method is to periodically perturb (i.e., adjust) the operating voltage or duty cycle of the PV system and observe the effect on output power. If the power output increases after the perturbation, the algorithm continues in the same direction; if the power decreases, the direction of the perturbation is reversed. This method works by sensing voltage and current from the PV array and calculating power in each iteration. The power is then compared with the previous power value. Based on this comparison, the algorithm decides whether to increase or decrease the voltage to reach the maximum power point. The algorithm is simple, cost-effective, and easy to implement in real-time embedded systems. However, it may introduce small oscillations around the maximum power point under stable conditions and can struggle under fast-changing environmental conditions such as rapidly varying irradiance as shown in Fig.5. Still, due to its balance between simplicity and performance, it is one of the most preferred MPPT techniques in solar PV applications.

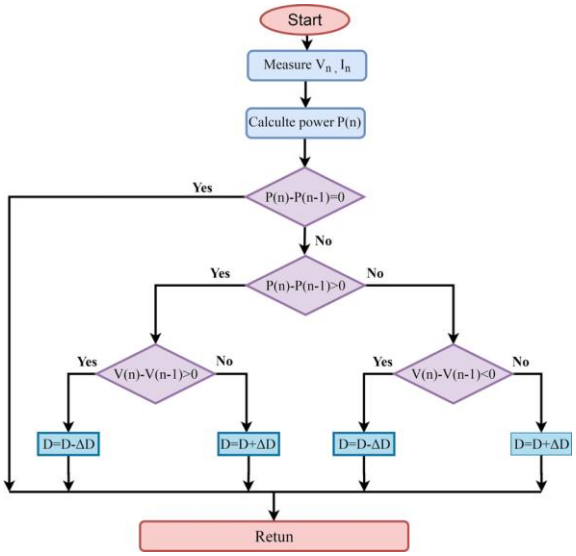

Fig.5 flow chart for P&O MPPT algorithm

4. Control Strategy of Grid-Side Bidirectional Voltage Source Converter

The grid-side bidirectional voltage source converter controls power flow between the DC link and the AC grid, allowing energy transfer in both directions. To simplify control, the three-phase AC voltages and currents are transformed into the rotating dq0 reference frame, which converts sinusoidal signals into steady DC values. The control system uses a double-loop structure, where the outer loop regulates the DC bus voltage by comparing it with a reference and adjusting the active power flow accordingly. This generates current references aligned with the d-axis for active power control. The inner loop ensures the actual grid currents track these reference currents by controlling the d-axis and q-axis currents, which correspond to active and reactive power, respectively, using proportional-integral

(PI) controllers. The PI controllers in both loops are critical for maintaining accurate and stable control by minimizing steady-state errors and providing a fast dynamic response. The controller also includes the grid voltage expressed in the dq0 frame to maintain synchronization between the converter and the grid. Additionally, the system compensates for the voltage drop caused by the inductance and switching frequency by including a term based on the product of the angular frequency (ω), inductance (L), and current (I), often referred to as the ωLc component. This compensation helps decouple the d-axis and q-axis controls, reducing interference between them and improving the dynamic response and stability of the system as shown in Fig.6. By integrating the grid voltage in dq0 form, the ωLc compensation, and using PI controllers in both the voltage and current loops, the control strategy achieves precise regulation of active and reactive power, maintains power quality, and ensures reliable operation of the converter in grid-connected applications.

1. dq0 Transformation of Grid Voltages and Currents

The three-phase voltages (va,vb,vc) and currents (ia,ib,ic) are transformed into the dq0 reference frame:

$$\begin{bmatrix} v_d \\ v_q \\ v_0 \end{bmatrix} = \frac{2}{3} \begin{bmatrix} \cos\theta & \cos\left(\theta - \frac{2\pi}{3}\right) & \cos\left(\theta - \frac{2\pi}{3}\right) \\ -\sin\theta & -\sin\left(\theta - \frac{2\pi}{3}\right) & -\sin\left(\theta + \frac{2\pi}{3}\right) \\ \frac{1}{2} & \frac{1}{2} & \frac{1}{2} \end{bmatrix} \begin{bmatrix} v_a \\ v_b \\ v_c \end{bmatrix} \quad (14)$$

Similarly for currents id,iq,i0

2. Voltage Equations of the VSC with ωLc Compensation

The converter voltage references vd∗ and vq∗ for the PWM generation are computed as:

$$V_d^* = v_d^{\text{grid}} - \omega L i_q + L\frac{di_d}{dt} + Ri_d + v_d^{PI} \quad (15)$$

$$V_q^* = v_q^{\text{grid}} - \omega L i_d + L\frac{di_q}{dt} + Ri_q + v_q^{PI} \quad (16)$$

Where:

- V_d^*, V_q^* are the reference voltages applied to the converter.
- v_d^{grid} , v_q^{grid} are the dq components of the grid voltage.
- R is the resistance of the filter
- L is the inductance of the filter
- i_d, i_q are the dq components of the grid current.
- $\frac{di_d}{dt}$, $\frac{di_q}{dt}$ are the derivatives of the dq currents.
- ω is the angular frequency of the grid.
- v_d^{PI}, v_q^{PI} are the output of the PI controller for current control.

The terms ωLi represent the ωLc compensation that decouples the d- and q-axis currents.

3. Outer Loop: DC Voltage Control

The DC bus voltage error:

$$e_{V_{dc}} = V_{dc}^{ref} - V_{dc} \quad (17)$$

The PI controller output generates the d-axis current reference idref:

$$i_d^{ref} = k_p^V e_{V_{dc}} + K_i^V \int e_{V_{dc}} dt \quad (18)$$

Where k_p^V and K_i^V are proportional and integral gains of the DC voltage PI controller.

4. Inner Loop: Current Control

The current errors in dq axes:

$$e_{i_d} = i_d^{ref} - i_d \quad (19)$$

$$e_{i_q} = i_q^{ref} - i_q \quad (20)$$

The PI controllers for current regulate voltages v_d^{PI} and v_q^{PI}:

$$v_d^{PI} = K_p^i e_{i_d} + K_i^i \int e_{i_d} dt \quad (21)$$

$$v_q^{PI} = K_p^i e_{i_q} + K_i^i \int e_{i_q} dt \quad (22)$$

Where K_p^i and K_i^i are the proportional and integral gains for the current PI controllers.

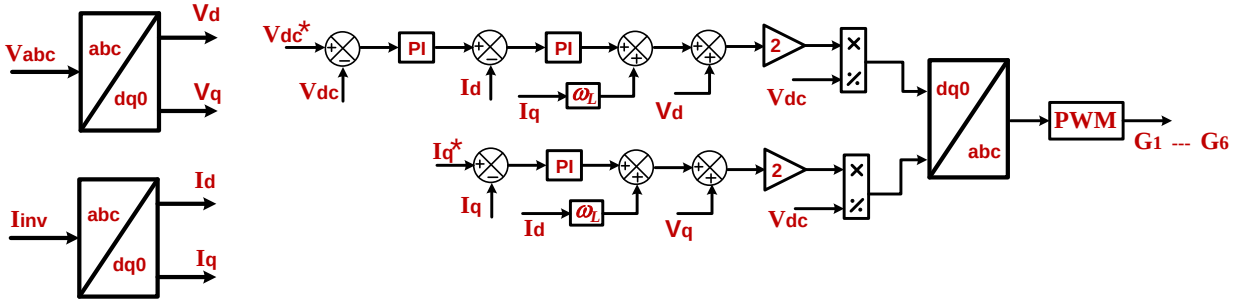

Fig. 6 Grid conversion controller

5. Combined Wireless Power Transfer and Auxiliary Power Module for Dual Battery charging configuration

The proposed integration method presents an advanced power delivery architecture that combines a solar and grid-based input supply with a wireless power transfer system and an auxiliary power module. This setup effectively charges both high voltage and low voltage batteries in electric vehicles. It uses a shared power electronic converter and a magnetic coupler within a double sided LCC LCC resonant topology to achieve high efficiency energy transfer at a designed resonant frequency omega zero. The input power is derived from both photovoltaic solar generation and the utility grid. This hybrid source feeds a power factor correction converter which delivers a stable and regulated DC link voltage. This DC voltage is supplied to a full bridge inverter consisting of switches S1 to S4, which produces an alternating current waveform to excite the primary side LCC resonant network. The resonant power is magnetically coupled through the shared transformer to the secondary side, where two separate full bridge rectifiers, one with switches S5 to S8 for the high voltage battery and another with switches S9 to S12 for the low voltage battery, convert the received power back to direct current. The auxiliary power module transformer is integrated within the compensation inductor path, enabling additional power transfer to the low voltage battery through mutual inductance. In Mode One, with the relay in the open state, both the wireless power transfer system and the auxiliary power module operate together, allowing simultaneous charging of both batteries. Power delivery is controlled using phase shift modulation, and zero voltage switching is achieved to minimize switching losses and improve efficiency. In Mode Two, with the relay closed, only the auxiliary power module remains active, using energy from the high voltage battery to charge the low voltage battery. In this mode, the resonant capacitor on the low voltage side is short circuited to reduce the voltage and enable accurate voltage regulation through phase shift control as shown in Fig.7. The system maintains impedance matching and high conversion efficiency. This integrated structure maximizes the use of solar and grid resources and enables compact, flexible, and efficient power delivery suitable for electric vehicles with dual battery systems.

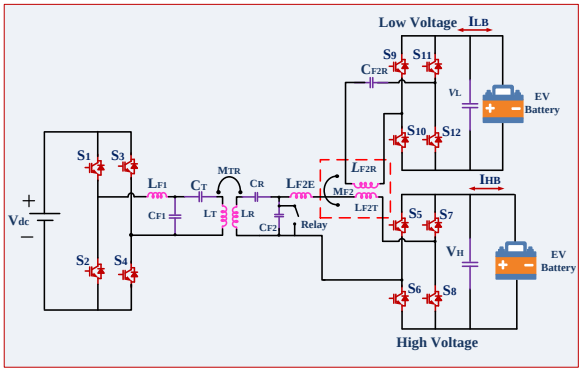

Fig. 7. Proposed integrated topology of WPT and APM.

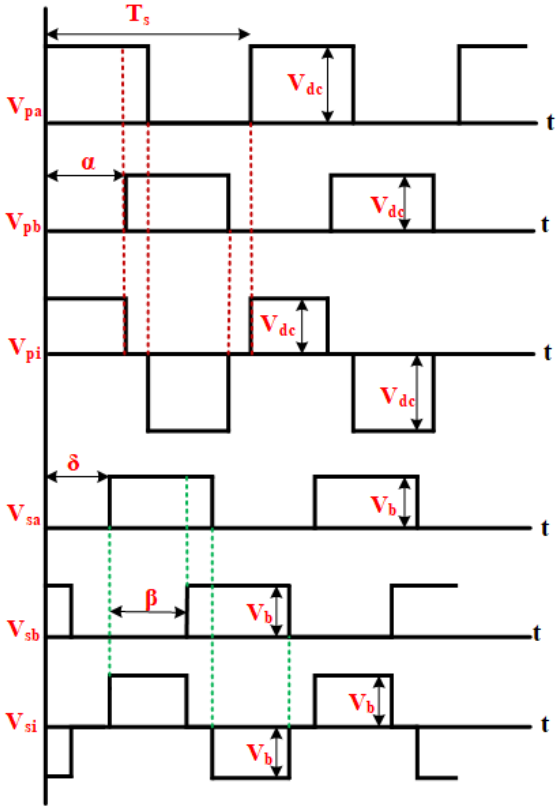

Fig. 8 switching waveforms of BWPT for V2G and G2V Operation

A. Grid and Solar to HV Battery Charging Formulas (LCC-WPT-Based)

1. Inverter Output Voltage:

$$U_T = \frac{2\sqrt{2}}{\pi} V_{INV} \qquad (23)$$

V_{INV}: DC-link voltage after PFC stage (from solar + grid)

2. Primary LCC Compensation Impedance:

$$Z_{LCC1} = j\omega L_{F1} + \frac{1}{j\omega C_{F_1}} + \frac{1}{\frac{1}{j\omega C_T} + \frac{1}{Z_{coi\_eq}}} \qquad (24)$$

Where:

- LF1,CF1,CT: primary filter inductor, parallel capacitor, series capacitor
- Zcoil_eq: reflected impedance of secondary coil

3. Secondary Side Impedance Matching (LCC)

$$Z_{secondary} = j\omega L_{f2} + \left(\frac{1}{j\omega C_{f_2}} \| \left(j\omega L_R + \frac{1}{j\omega C_R}\right)\right) \quad (25)$$

At resonance:

$$\omega^2 = \frac{1}{L_R C_R} \quad (26)$$

$$\omega^2 = \frac{1}{L_{f^2} C_{f^2}} \quad (27)$$

So secondary behaves as resistive load Rload

4. Mutual Inductance Model (WPT):

$$Z_{in} = j\omega L_T + \frac{\omega^2 M^2}{Z_{\text{sec}}} \quad (28)$$

$$Z_{\text{sec}} = j\omega L_R + \frac{1}{j\omega c_R} + R_{Load} \quad (29)$$

- M: mutual inductance between coils
- LT, LR: primary and secondary coils
- CR: compensation capacitor on secondary side
- Rload: reflected load of HV battery + rectifier + filters

5. Resonance Frequency (Double-Sided LCC Matching):

For both sides to operate in resonance:

$$\omega_0 = \frac{1}{\sqrt{L_{F_1} C_{F_1}}} = \frac{1}{\sqrt{L_T C_T}} = \frac{1}{\sqrt{L_R C_R}} = \frac{1}{\sqrt{L_{F_2} C_{F_2}}} \quad (30)$$

- Ensures Zero Voltage Switching (ZVS) and maximum power transfer.

6. Power Transferred Through Magnetic Link to HV Battery:

$$P_{HV} = \frac{\omega^2 M^2 V_{inv}^2}{R_{eq2} \cdot \left((R_{eq1} + R_T)^2 + \left(\omega L_{eq} - \frac{1}{\omega C_{eq}}\right)^2 \right)} \quad (31)$$

Where:

- Req2: Equivalent resistance on secondary side
- Vinv: Inverter output (fundamental)

7. Reflected Load Impedance to Primary Side:

$Z_{refl} = \left(\frac{\omega M}{Z_{sec}}\right)^2$ (use this in series with L_T in Z_{in}) (32)

8. Input Power (from Grid + Solar via Inverter):

$$P_{in} = \frac{V_{INV}^2}{Z_{LCC1}^{total}} \quad (33)$$

Z_{LCC1}^{total} total equivalent impedance of the primary LCC stage and reflected load

9. Equivalent Load at Secondary Side (After Rectifier & Filter):

$$R_{eq\_dc} = \frac{V_{HV}^2}{P_{HV}} \Rightarrow R_{eq\_ac} = \frac{8}{\pi^2} R_{eq\_dc} \quad (34)$$

B. LV Battery Charging via WPT + APM (Shared Path)

The LV battery is charged through shared magnetic coupling with APM transformer tap on the secondary side.

1. Inverter to Secondary APM Voltage Induction:

$$V_L \approx \frac{M_{F2} \cdot V_{inv}}{L_{F2}} \quad (35)$$

Where:

- MF2: Mutual inductance of APM transformer branch
- LF2: Inductance in the secondary compensating path

2. LV Side Current via WPT-Auxiliary Branch:

$$I_{F2R} = \frac{U_H \cdot \left(\frac{R_{EQ2} L_{F2}}{M_{F2}}\right)}{\left(\frac{R_{EQ2} L_{F2}}{M_{F2}}\right)^2 + (\omega M_{F2})^2} \quad (36)$$

- UH is the AC voltage derived from HV line
- REQ2: Equivalent load resistance for LV battery path

3. LV Output Voltage:

$$V_L \approx \frac{M_{F2} \cdot V_{HV}}{L_{F2}} \quad (37)$$

4. LV Battery Charging Power:

$$P_{LV} = \frac{64 R_{L2} V_{HV}^2}{(\pi^2 \omega M_{F2})^2 + \left(\frac{8 R_{L2} L_{F2}}{M_{F2}}\right)^2} \quad (38)$$

5. **LV Battery Charging Current:**

$$I_{LV} = \frac{P_{LV}}{V_L} \quad (39)$$

6. Simulation Results and discussion

A. Dynamic Power Management of Solar and Grid Integrated wireless Power Transfer in Hybrid Charging Setup

The proposed bidirectional wireless power transfer (WPT) system integrated with a hybrid solar-grid framework was simulated in MATLAB/Simulink over a total runtime of 1 second to analyze dynamic power flow behavior under varying generation and load conditions. The system was designed with a 10 kW solar photovoltaic (PV) array, a 230 V, 50 Hz grid connection, and electric vehicle (EV) batteries comprising a 20 kW high-voltage (HV) pack and a 15 kW low-voltage (LV) pack. A common DC-link maintained at 380 V ensured stable energy transfer between sources and loads. The wireless energy transfer path and auxiliary power module (APM) supported bidirectional flow and real-time power balancing between grid and solar sources to meet EV charging demands. During the initial interval from 0 to 0.2 seconds, solar irradiance was zero (0 W/m²), resulting in no power generation from the PV system. Consequently, the full 15 kW EV battery load was met entirely by the grid through the WPT interface, demonstrating the grid's ability to handle peak load

independently. Between 0.2 and 0.45 seconds, solar irradiance increased to 500 W/m², allowing the PV system to generate approximately 5 kW. During this period, the grid contributed the remaining 10 kW to fulfill the constant 15 kW EV demand, illustrating effective hybrid operation and partial load sharing. From 0.45 to 1 second, solar irradiance ramped up to 1000 W/m², enabling the PV system to reach its rated capacity of 10 kW. As a result, the grid input reduced proportionally to supply only 5 kW of the required energy, while the remaining 10 kW was delivered wirelessly from the solar source. This period confirmed the system's dynamic balancing capability between solar and grid input, governed by real-time energy availability. Furthermore, from 0.6 to 0.8 seconds, the EV battery load decreased from 15 kW to 12.5 kW. In this condition, the 10 kW solar generation was sufficient to meet the majority of the EV load, while the surplus solar energy was redirected to the grid through the bidirectional interface, highlighting the backflow capability and grid-supportive operation. Finally, in the interval from 0.8 to 1 second, the EV battery load dropped to 0 kW, indicating a fully charged state. The complete 10 kW generated by the solar array was then transferred back to the grid, demonstrating seamless transition from load support to energy export mode. This dynamic power management scenario, illustrated in Fig. 9, confirms the effectiveness of the proposed system in intelligently coordinating solar and grid power sources while adapting to real-time load variations. The simulation results validate the system's robust control strategy, efficient energy utilization, and bidirectional transfer capability, making it suitable for resilient and flexible EV charging infrastructure.

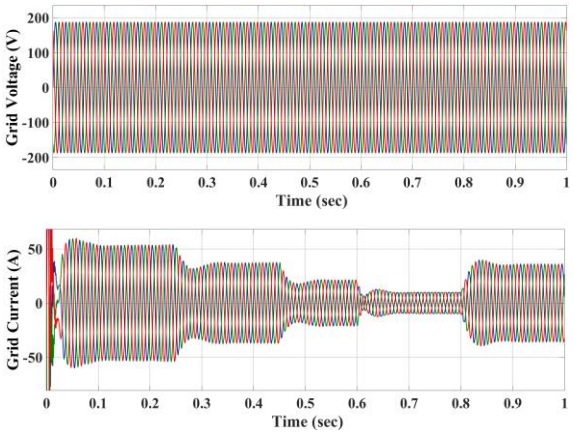

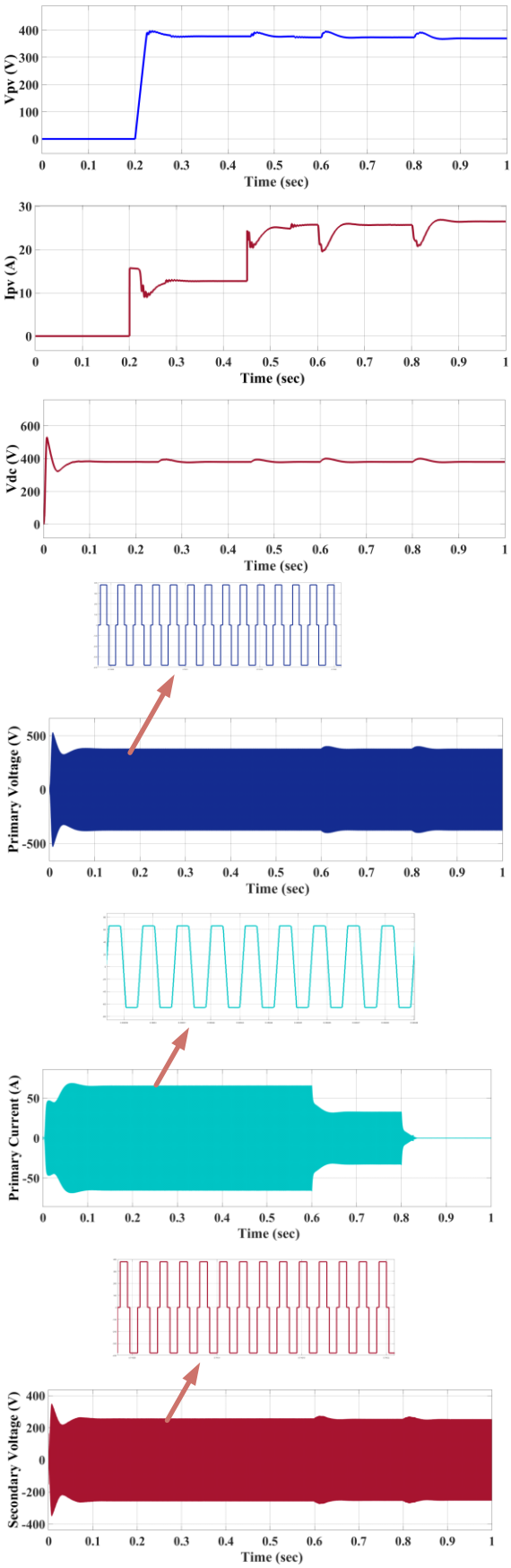

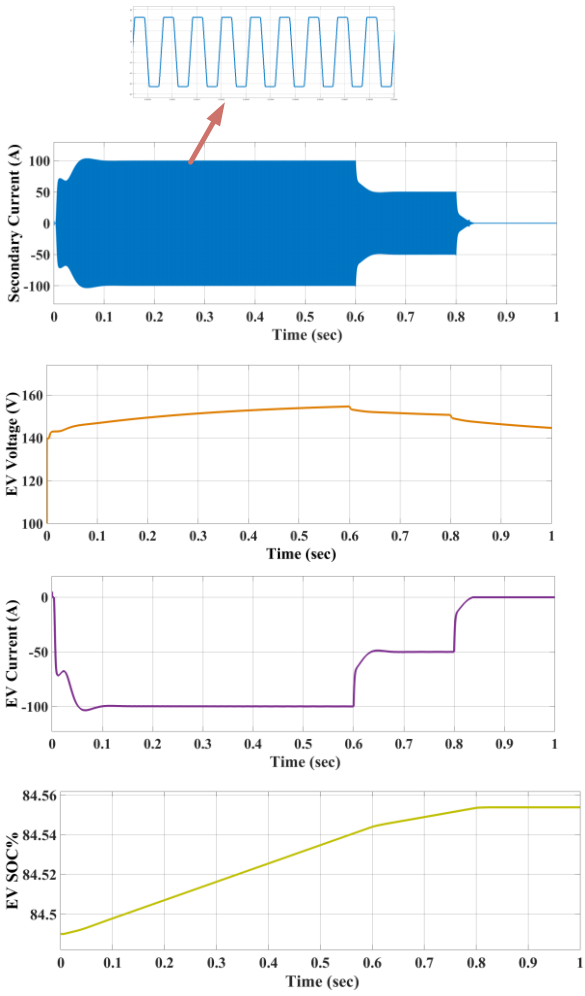

Fig.9 Simulation results of grid connected solar PV system for EV charging

B. Power Management Behavior of the Proposed EV Charging System

The proposed bidirectional wireless power transfer (WPT) system, integrated with a hybrid solar and grid-based architecture, was simulated to evaluate its real-time power balancing capability under dynamically changing load and generation conditions. The system includes solar photovoltaic generation, a grid interface, and two EV battery packs connected via a DC-link. At the start of the simulation, solar generation was inactive, and the grid met the entire EV charging demand. As solar irradiance increased, the photovoltaic array began contributing power to the EV load, leading to a reduction in grid supply. This transition marked the onset of hybrid operation, where both solar and grid sources collaboratively fulfilled the EV charging requirements as shown in Fig.10. As solar generation increased, the photovoltaic system became dominant, and the grid supply was minimized, demonstrating the system's ability to prioritize renewable energy. The bidirectional nature of the WPT and APM architecture enabled the excess solar power to be redirected back to the grid when the EV load decreased.

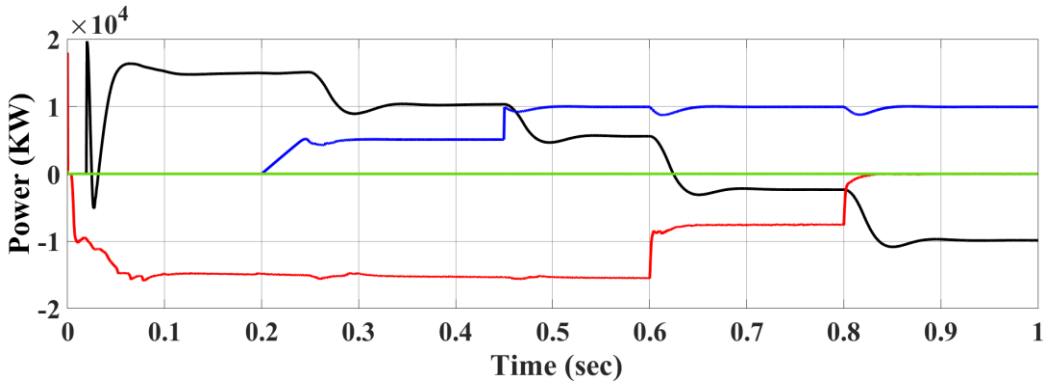

Fig. 10 simulation results of dynamic power management in grid connected solar PV system for EV charging

C. Battery-to-Battery Wireless Power Transfer Operation Using WPT and APM

In this scenario, a bidirectional battery-to-battery energy transfer is achieved wirelessly from the High Voltage (HV) EV battery to the Low Voltage (LV) EV battery through a shared magnetic coupler and Auxiliary Power Module (APM). The system is simulated in MATLAB for total time duration of 1 second. From 0 to 0.2 seconds, the LV battery begins charging with a power intake of 5 kW, while the HV battery simultaneously discharges 5 kW to support this demand. As the simulation progresses, a gradual reduction in power transfer is observed. Between 0.2 and 0.4 seconds, the charging power to the LV battery decreases to 4.5 kW, with a matching discharges from the HV battery. This downward trend continues from 0.4 to 0.6 seconds, where the transferred power is 3 kW, followed by 2.5 kW during 0.6 to 0.8 seconds, and finally reducing to 1

kW from 0.8 to 1 second. This controlled decrement in power flow illustrates the dynamic and flexible operation of the WPT-enabled APM, enabling efficient power sharing and voltage-level adaptation between different EV battery systems. The simulation confirms the system's ability to maintain safe and synchronized bidirectional wireless energy transfer under varying load and discharge conditions, as shown in Fig. 11.

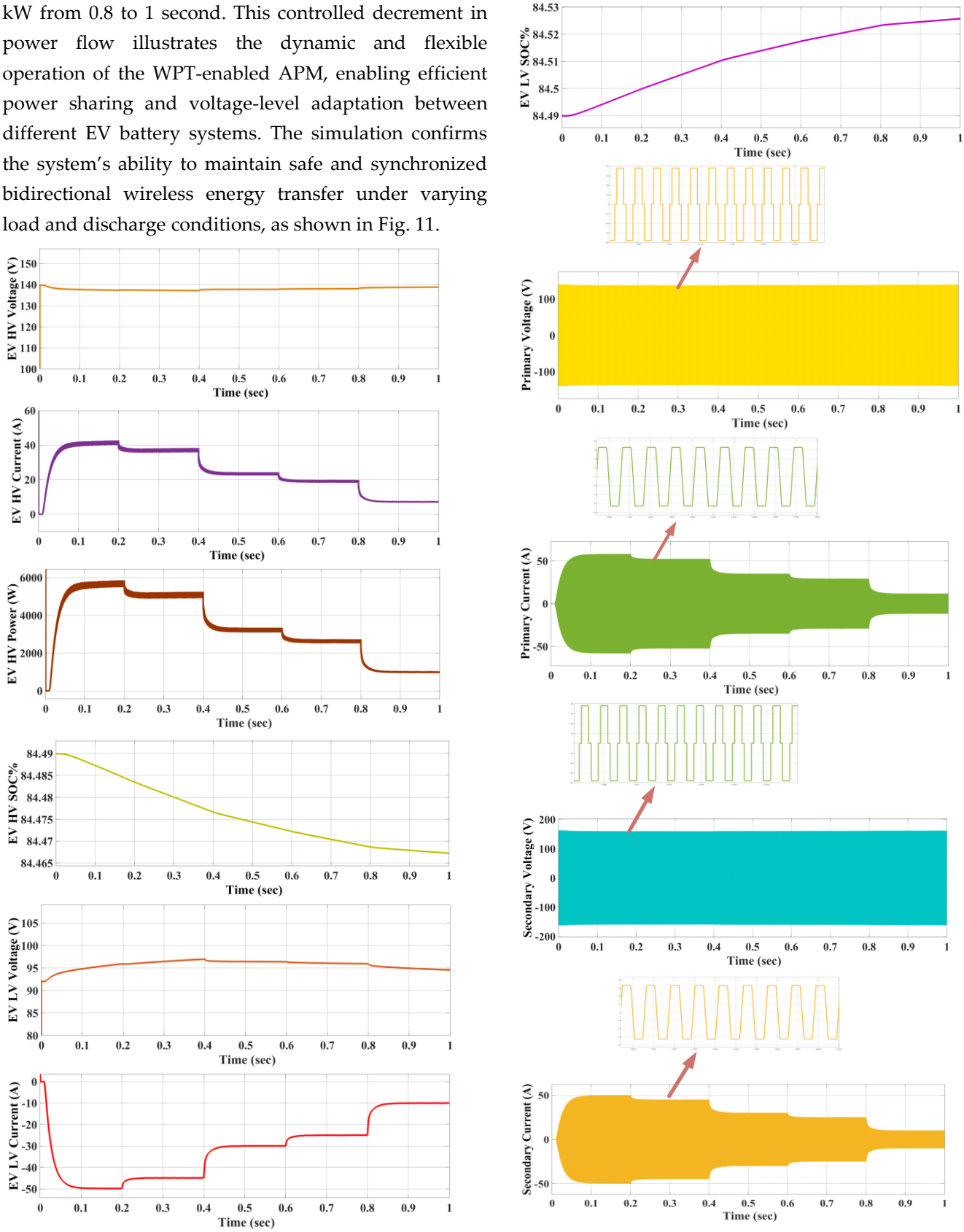

Fig.11 Dynamic EV battery to battery wireless power transfer operation using WPT and APM

7. Conclusion

This paper proposes a combined wireless power transfer and auxiliary power module system for dual battery

charging in electric vehicles, integrating both high-voltage and low-voltage battery packs within a hybrid solar-grid energy framework. Utilizing a shared power converter and magnetic coupler in a double-sided LCC resonant topology, the system efficiently delivers power at the resonant frequency with effective impedance matching and minimal switching losses. The integration of solar PV with MPPT maximizes renewable energy extraction, while the bidirectional voltage source converter ensures grid stability and power quality. The auxiliary power module facilitates flexible energy exchange between the dual batteries, supporting simultaneous or independent charging modes through phase-shift control and zero voltage switching techniques. Simulation results demonstrate that the proposed combined wireless power transfer and auxiliary power module architecture enables efficient, compact, and flexible dual battery charging with reduced grid dependency and enhanced system resilience. This approach offers a promising solution for sustainable and reliable EV charging infrastructure, including off-grid and emergency scenarios.

Conflict of interest statement

Authors declare that they do not have any conflict of interest.

REFERENCES

[1] M. B. Hossain, M. R. Islam, K. M. Muttaqi, D. Sutanto, and A. P. Agalgaonkar, ''Advancement of fuel cells and electrolyzers technologies and their applications to renewable-rich power grids,'' J. Energy Storage, vol. 62, Jun. 2023, Art. no. 106842.

[2] M. Tavassoli and A. Kamran-Pirzaman, ''Comparison of effective greenhouse gases and global warming,'' in Proc. 8th Int. Conf. Technol. Energy Manage. (ICTEM), Feb. 2023, pp. 1–5.

[3] R. T. Jacob and R. Liyanapathirana, ''Technical feasibility in reaching renewable energy targets; case study on Australia,'' in Proc. 4th Int. Conf. Electr. Energy Syst. (ICEES), Feb. 2018, pp. 630–634.

[4] N. Winter, ''Renewables 2023 global status report collection economic & social value creation employment factsheet,'' REN21, Paris, France, 2023. Accessed: Jul. 22, 2024.

[5] N. Hou and Y.W. Li, ''Overview and comparison of modulation and control strategies for a nonresonant single-phase dual-active-bridge DC–DC converter,'' IEEE Trans. Power Electron., vol. 35, no. 3, pp. 3148–3172, Mar. 2020.

[6] B. Zhao, Q. Song, W. Liu, and W. Sun, ''Current-stress-optimized switching strategy of isolated bidirectional DC–DC converter with dual-phase-shift control,'' IEEE Trans. Ind. Electron., vol. 60, no. 10, pp. 4458–4467, Oct. 2013.

[7] H. Bai and C. Mi, ''Eliminate reactive power and increase system efficiency of isolated bidirectional dual-active-bridge DC–DC converters using novel dual-phase-shift control,'' IEEE Trans. Power Electron., vol. 23, no. 6, pp. 2905–2914, Nov. 2008.

[8] F. Krismer and J.W. Kolar, ''Closed form solution for minimum conduction loss modulation of DAB converters,'' IEEE Trans. Power Electron., vol. 27, no. 1, pp. 174–188, Jan. 2012.

[9] F. Krismer and J. W. Kolar, ''Efficiency-optimized high-current dual active bridge converter for automotive applications,'' IEEE Trans. Ind. Electron., vol. 59, no. 7, pp. 2745–2760, Jul. 2012.

[10] B. Zhao, Q. Song, andW. Liu, ''Efficiency characterization and optimization of isolated bidirectional DC–DC converter based on dual-phase-shift control for DC distribution application,'' IEEE Trans. Power Electron., vol. 28, no. 4, pp. 1711–1727, Apr. 2013.

[11] J. Han, X. Zhou, S. Lu, and P. Zhao, ''A three-phase bidirectional gridconnected AC/DC converter for V2G applications,'' J. Control Sci. Eng., vol. 2020, Jan. 2020, Art. no. 8844073.

[12] M. Liserre, F. Blaabjerg, and S. Hansen, ''Design and control of an LCLfilter- based three-phase active rectifier,'' IEEE Trans. Ind. Appl., vol. 41, no. 5, pp. 1281–1291, Sep./Oct. 2005.

[13] F. Liu, X. Zhang, C. Yu, Z. Shao, W. Zhao, and H. Ni, ''LCL-filter design for grid-connected three-phasePWMconverter based on maximum current ripple,'' in Proc. IEEE ECCE Asia Downunder, Jun. 2013, pp. 631–635.

[14] K. Frisfelds and O. Krievs, ''Design of a three-phase bidirectional PWM rectifier with simple control algorithm,'' Latvian J. Phys. Tech. Sci., vol. 56, no. 3, pp. 3–12, Jun. 2019.

[15] G. Majic, M. Despalatovic, and B. Terzic, ''LCL filter design method for grid-connected PWM-VSC,'' J. Electr. Eng. Technol., vol. 12, no. 5, pp. 1945–1954, 2017.

[16] H. Arya and M. Das, "Solar powered EV fast charging station to support distribution grid," in Proc. IEEE 9th Int. Conf. Power Syst., 2021, pp. 1–6.

[17] Y. Liao and C. Lu, "Dispatch of EV charging station energy resources for sustainable mobility," IEEE Trans. Transp. Electrific., vol. 1, no. 1, pp. 86–93, Jun. 2015.

[18] V. T. Tran, M. R. Islam, K. M. Muttaqi, and D. Sutanto, "An efficient energy management approach for a solar-powered EV battery charging facility to support distribution grids," IEEE Trans. Ind. Appl., vol. 55, no. 6, pp. 6517–6526, Nov./Dec. 2019.

[19] A. Majzoobi and A. Khodaei, "Application of microgrids in supporting distribution grid flexibility," IEEE Trans. Power Syst., vol. 32, no. 5, pp. 3660–3669, Sep. 2017.

[20] I. Kougioulis, P. Wheeler, and M. R. Ahmed, "An integrated on-board charger and auxiliary power module for electric vehicles," in Proc. IEEE Appl. Power Electron. Conf. Expo., 2022, pp. 1162–1169.

[21] L. Zhu, H. Bai, A. Brown, and L. Keuck, "A current-fed three-port DC/DC converter for integration of on-board charger and auxiliary power module in electric vehicles," in Proc. IEEE Appl. Power Electron. Conf. Expo., 2021, pp. 577–582.

[22] C. C. D. Viana, M. Pathmanathan, and P. W. Lehn, "Auxiliary power module elimination in EVs using dual inverter drivetrain," IEEE Trans. Power Electron., vol. 37, no. 10, pp. 12513–12524, Oct. 2022.

[23] Y. Zhang et al., "Integration of onboard charger and wireless charging system for electric vehicles with shared coupler,

compensation, and rectifier," IEEE Trans. Ind. Electron., vol. 70, no. 7, pp. 7511–7514, Jul. 2023.

[24] G. Yu and S. Choi, "An effective integration of APM and OBC with simultaneous operation and entire ZVS range for electric vehicle," IEEE Trans. Power Electron., vol. 36, no. 9, pp. 10343–10354, Sep. 2021.

[25] R. Hou and A. Emadi, "A primary full-integrated active filter auxiliary power module in electrified vehicles with single-phase onboard chargers," IEEE Trans. Power Electron., vol. 32, no. 11, pp. 8393–8405, Nov. 2017.